[7] T. Gratieri and Y. Kalia, *Mathematical models to describe iontophoretic transport in vitro and in vivo and the effect of current application on the skin barrier*, Adv Drug Deliv Rev. **65** (2013), 315–329.
[8] T. Jaskari, M. Vuorio, K. Kontturi, A. Urtti, J. Manzanares, and J. Hirvonen, *Controlled transdermal iontophoresis by ion-exchanges fiber*, J Control Release **67** (2000), 179–190.
[9] A. Kaushik, R. Jayant, V. Sagar, and M. Nair, *The potential of magneto-electric nanocarriers for drug delivery*, Expert Opin Drug Deliv **11** (2014), 1–11.
[10] S. Molokhia, Y. Zhang, W. Higuchi, and S. Li, *Iontophoretic transport across a multiple membrane system*, J Pharma Sci **97** (2008), 490–505.
[11] R. Pignatello, M. Fresta, and G. Puglisi, *Transdermal drug delivery by iontophoresis. I. fundamentals and theoretical aspects*, J Appl Cosmetol **14** (1996), 59–72.
[12] K. Tojo, *Mathematical model of iontophoretic transdermal drug delivery*, J Chemical Eng Japan **22** (1989), 512–518.
[13] A. Yadollahpour and Z. Razaee, *Electroporation as a new cancer treatment technique: a review on the mechanisms of action*, Biomed Pharmacol J **7** (2014), 53–62.
[14] M. Yarmush, A. Golberg, G. Serša, T. Kotnik, and D. Miklavčič, *Electroporation-based technologies for medicine: principles, applications, and challenges*, Annu Rev Biomed Eng **16** (2014), 295–320.

J. A. Ferreira
CMUC, Department of Mathematics, University of Coimbra, Portugal
E-mail address: ferreira@mat.uc.pt

P. de Oliveira
CMUC, Department of Mathematics, University of Coimbra, Portugal
E-mail address: poliveir@mat.uc.pt

G. Pena
CMUC, Department of Mathematics, University of Coimbra, Portugal
E-mail address: gpena@mat.uc.pt

Pré-Publicações do Departamento de Matemática
Universidade de Coimbra
Preprint Number 16–03

TRANSDERMAL IONTOPHORESIS - A QUANTITATIVE AND QUALITATIVE STUDY

J. A. FERREIRA, P. DE OLIVEIRA AND G. PENA

Abstract: The use of enhancers to increase the drug molecules penetration into target tissues is an usual technique in drug delivery. In transdermal drug delivery, electric fields are often used to increase the drug transport through the skin. In this paper we study a drug delivery mechanism from a reservoir which is in contact with the skin. We assume that the drug transport in the coupled system is enhanced by a small electric field that induces a convective field. We establish energy estimates for the coupled system and we propose a semi-analytical discrete coupled model that mimics the continuous model. The qualitative behaviour of the system is illustrated.

Keywords: Iontophoresis, mathematical model, numerical simulation.

1. Introduction

Intelligent drug delivery devices have been developed during the last decades to deliver drugs in a controlled manner at specific locations. Some of these systems use stimuli-responsive polymers (where the drug is entrapped) that are able to respond to the modification of the external environment (like electric fields, pH and temperature). Electric fields are an interesting type of stimulus because they can be precisely controlled, and the drug delivery responses can be predicted.

The use of electric fields as enhancers is popular in transdermal drug delivery where iontophoresis ([1, 5, 7, 8, 10, 12]) and electroporation ([1, 3, 4, 14]) or a combination of both, are usual procedures. Drug delivery systems for cancer treatment based on this technology were recently developed ([13]). In this case, the device based on drug-encapsulated nanoparticles is remotely controlled by an electric field to deliver the biological agent in the cancer target tissue (electrochemotherapy, see [9]). Each of the above applications involves complex phenomena. For instance, in transdermal drug delivery, enhanced by an electric field, the drug and its solvent vehicle leaves the polymeric matrix, enters the stratum corneum and is transported through

Received February 22nd, 2016.
This work was partially supported by the Centre for Mathematics of the University of Coimbra - UID/MAT/00324/2013, funded by the Portuguese Government through FCT/MEC and co-funded by the European Regional Development Fund through the Partnership Agreement PT2020.

the skin to reach the circulatory system. In both media, the transport occurs by passive diffusion, electromigration (migration of ions due to the electric field) and electroosmosis (transport due the solvent movement) ([7, 11, 12]).

In an iontophoresis procedure, a small electric field is applied to the coupled system to enhance the drug transport. If the drug molecules are positively charged, then the anode is in contact with the reservoir and the cathode is in the opposite position. The anode will repel the positively charged drug into the skin. If the drug is negatively charged it will be placed under the cathode that will repel it into the skin.The generated electric field induces a convective flux in the system that depends on the drug molecules valence, intensity of the electric field, temperature, electric conductivity of both media and drug diffusion ([7, 8]). In this case, the anode is called the active electrode and the cathode the passive electrode.

We are interested in studying transdermal iontophoretic applications consisting of a coupled system having a reservoir containing a charged drug and a tissue, see Figure 1.

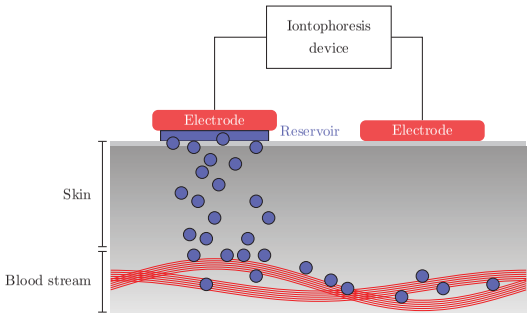

FIGURE 1. Drug delivery system for the skin enhanced by an electric potential.

In this case, the polymeric reservoir is in contact with the skin which is a multilayered tissue: epidermis ($100\mu m$), dermis ($2-3mm$) and subcutaneous tissue. These three layers have different hystological characteristics and functions, however, to simplify the mathematical model, we represent the skin as one layer. The electric field is generated by a potential of low intensity applied during long periods of time. The drug transport occurs by passive diffusion and convection caused by the potential gradient.

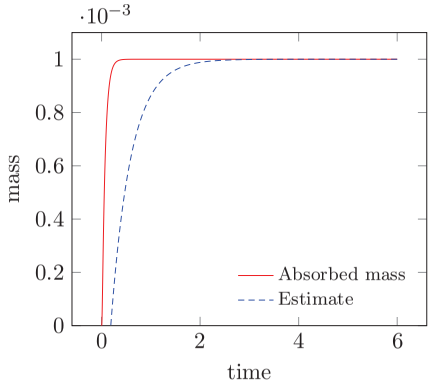

FIGURE 5. Illustration of the absorbed mass lower bound (44).

The convection-diffusion drug system was studied and its stability was concluded under different assumptions on the parameters of the model. The energy estimates were used to obtain estimates for the drug in the coupled system and for the released drug. Such estimates can be used to design iontophoretic systems with a prescribed behaviour.

A numerical method that mimics the continuous model was proposed. The discrete interface conditions induces difficulties in the stability analysis. To avoid such problems a convenient L^2 discrete norm and seminorm were introduced and a discrete Poincaré inequality was proved. These ingredients were crucial to establish discrete energy estimates for an implicit method. The qualitative behaviour of the numerical solutions was explored.

References

[1] A. Banga, S. Bose, and T. Ghosh, *Iontophoresis and electroporation: comparisons and contrasts*, Int J Pharma **179** (1999), 1–19.

[2] S. Barbeiro and J. A. Ferreira, *Coupled vehicle-skin models for drug release*, Computer Meth Appl Mech Engrg **198** (2009), 2078–2086.

[3] S. Becker, *Transport modelling of skin electroporation and thermal behaviour of the stratum corneum*, Int J Therm Sci **54** (2012), 48–61.

[4] S. Becker, B. Zorec, D.Miklavčič, and N. Pavšelj, *Transdermal transport pathway creation: electroporation pulse order*, Math Biosc **257** (2014), 60–68.

[5] N. Dixit, V. Bali, S. Baboota, A. Ahuja, and J. Ali, *Iontophoresis - an approach for controlled drug delivery: a review*, Current Drug Delivery **4** (2007), 1–10.

[6] J. A. Ferreira, M. Lauricella, G. Pena, and G. Pontrelli, *Iontophoretic transdermal drug delivery: a multi-layered approach*, 2016, arXiv:1601.03074.

$\delta\phi$	σ_r	$M_{\delta\phi}(6)$	$\frac{M_{\delta\phi}(6)-M_0(6)}{M_0(6)}$
0	-	$9.952 \cdot 10^{-4}$	0
0.02	0.015	$9.976 \cdot 10^{-4}$	0.00241157
	0.15	$9.959 \cdot 10^{-4}$	$6.83 \cdot 10^{-4}$
	1.5	$9.955 \cdot 10^{-4}$	$3.11 \cdot 10^{-4}$
0.2	0.015	$9.999997 \cdot 10^{-4}$	0.00483162
	0.15	$9.985957 \cdot 10^{-4}$	0.0034209
	1.5	$9.963522 \cdot 10^{-4}$	0.00116656
0.5	0.015	10^{-3}	0.00483194
	0.15	$9.99788 \cdot 10^{-4}$	0.00461911
	1.5	$9.96953 \cdot 10^{-4}$	0.0017705
2	0.015	10^{-3}	0.00483194
	0.15	$9.9999999994 \cdot 10^{-4}$	0.00483194
	1.5	$9.9872902264 \cdot 10^{-4}$	0.00355482

TABLE 1. Behaviour of the total mass absorbed for six hours, $M_{\delta\phi}(6)$

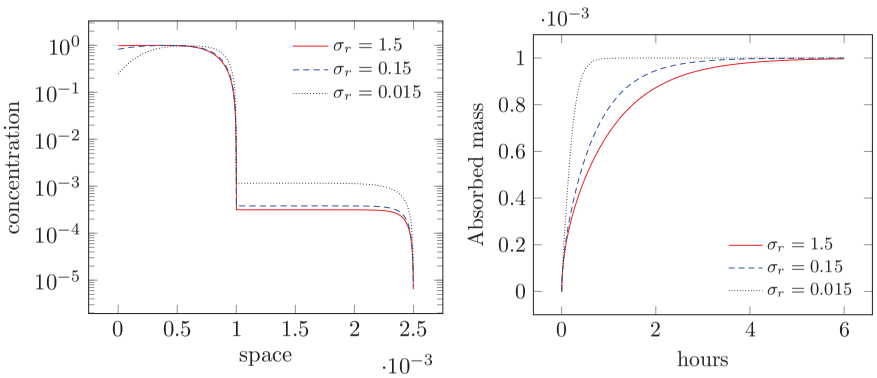

FIGURE 4. Drug concentration in the coupled system, after 6 hours (left) and absorbed mass during the 6 hours of treatment (right), for $\sigma_s = 0.015$, $\delta\phi = 0.5$.

The main goal of this paper is the study of a mathematical model that describes the drug transport through the reservoir and the target tissue, under the effect of an electric field. The considered model is a two-layer simplification of the multi-layered model introduced in [6], in the case of a perfect contact between reservoir and skin. The paper is organized as follows. In Section 2 we present the coupled mathematical model. Solving the coupled problem for the electric field, the convective field is explicitly given and the Laplace-drug equations are replaced by convection-diffusion equations. Energy estimates are obtained in Section 3. Such estimates are used to obtain lower bounds for the released drug. A numerical method that mimics the qualitative behaviour of the continuous model is introduced and studied in Section 4. In Section 5 we present some numerical results illustrating the behaviour of the coupled system in different scenarios. In Section 6 some conclusions are presented.

2. The Laplace-drug equations

In what follows we assume that the reservoir and the target tissue are isotropic media. This assumption allows the replacement of the 3D physical model, reservoir in contact with the target tissue, by a 1D model. Let $[0, \ell_1]$ be the reservoir and $(\ell_1, \ell_2]$ the target tissue layer. We assume that the left hand side of the reservoir is isolated and the drug molecules that attain the boundary $x = \ell_2$ are immediately removed. In the domains $(0, \ell_1)$ and (ℓ_1, ℓ_2) a diffusion process takes place enhanced by the electric field generated by the applied electric potential $\phi(V)$ at $x = 0$ and $x = \ell_2$, respectively, ϕ_0 and ϕ_1. We assume that the polymeric matrix of the reservoir and the target tissue have different electric conductivities σ_r and σ_s (S/m), respectively. We also assume that the diffusion coefficients of the drug in both media are represented, respectively, by D_r and D_s (m^2/s).

The drug transport in the polymeric matrix occurs by passive diffusion and convection induced by the electric field $E = -\nabla\phi$. Let J_r be the drug mass flux. By the Nernst-Planck equation we have

$$J_r = -D_r \nabla c_r - v_r c_r, \tag{1}$$

where c_r denotes the drug concentration (g/m^3) in the polymeric matrix and v_r (m/s) stands for the mean velocity of the solvent vehicle in the reservoir. Let J_s represent the drug mass flux in the skin. By the Nernst-Planck

equation we have

$$J_s = -D_s \nabla c_s - v_s c_s + v_{sol} c_s, \tag{2}$$

where c_r denotes the drug concentration in the target tissue. The convective velocity v_{sol}, caused by the electric field, represents the average velocity of the solvent vehicle.

The convective velocities v_k, $k = r, s$, are given by the Nernst-Einstein equation

$$v_r = \frac{D_r z F}{RT_r} \nabla \phi_r, \qquad v_s = \frac{D_s z F}{RT_s} \nabla \phi_s - v_{sol},$$

where z denotes the valence of the drug molecules, R the Faraday constant ($9.6485 \times 10^4 Coulomb/mol$), T_i the temperature (K) in the medium i, and R de gas constant ($8.31446 J/(Kmol)$).

We assume that the electric field is generated by applying low potentials during long periods of time. In these circumstances, the potential is described by the Laplace equation. As both media present different conductivity properties, two Laplace equations should be considered coupled with the convection-diffusion equations for the drug transport. From the previous considerations, the electric potentials in the reservoir, ϕ_r, and the skin, ϕ_s, are described by the two equations

$$\begin{cases} \sigma_r \Delta \phi_r = 0 \text{ in } (0, \ell_1) \\ \phi_r(0) = \phi_0, \end{cases} \tag{3}$$

and

$$\begin{cases} \sigma_r s \Delta \phi_s = 0 \text{ in } (\ell_1, \ell_2) \\ \phi_s(\ell_2) = \phi_1, \end{cases} \tag{4}$$

coupled with the transition condition

$$\begin{cases} \phi_r(\ell_1) = \phi_s(\ell_1) \text{ (continuity of the potential)} \\ \\ \sigma_r \nabla \phi_r(\ell_1) = \sigma_s \nabla \phi_s(\ell_1) \text{ (continuity of the electric field).} \end{cases} \tag{5}$$

We note that condition $\phi_s(\ell_2) = \phi_1$, in (4), represents an approximation of the real experimental condition. The potential ϕ_s is not applied in ℓ_2 - the interface between the skin and the blood system - but at the passive electrode.

The time-space drug evolution is described by the mass conservation law

$$\frac{\partial c_k}{\partial t} + \nabla \cdot J_k = 0, \; k = r, s,$$

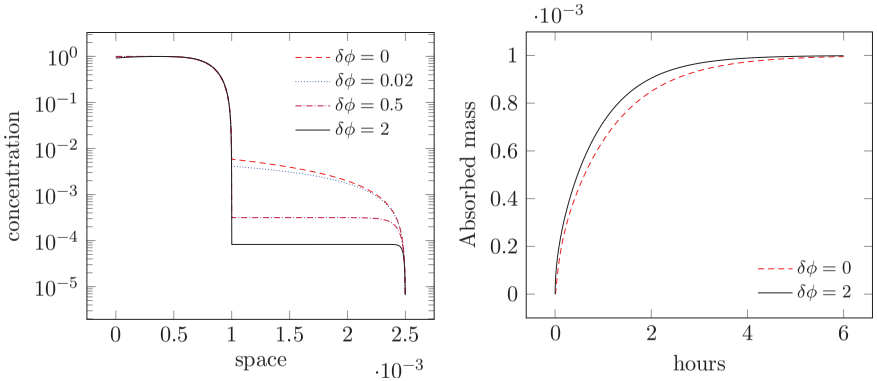

FIGURE 3. Drug concentration in the coupled system, after 6 hours (left) and absorbed mass during the 6 hours of treatment (right), for $\sigma_r = 1.5$, $\sigma_s = 0.015$.

Figures 3 and 4 (right) suggest that the reservoir's conductivity has a large influence, on the total amount of released drug, than the potential $\delta\phi$. A number of simulations that has been carried on Table 1 which clarifies the dependence of the total mass of absorbed over six hours, on the conductivity σ_r and the potential $\delta\phi$. In these tables, $M_0(6)$ represents the total mass absorbed when $\delta\phi = 0$. The influence of σ_r explains why polymeric conductivity is a major concern for manufacturers.

We finally present how estimate (44) can be useful. In Figure 5 we plot the real absorbed mass, as well as lower bound (44), which can be used to design protocols for drug delivery in this context. The parameters chosen for this particular simulation are $D_s = D_r = 10^{-8}$, $\delta\phi = 0.02$ and $\sigma_r = 0.15$. The remaining parameters are taken as in the previous simulations.

6. Conclusion

In this paper the mathematical model that describes the drug evolution in the coupled reservoir-target tissue is studied when the drug transport is enhanced by an applied electric field. We assume that the applied potential is stationary and is described by a coupled system that admits an explicit solution. As the electric field generates a convective field, the drug transport occurs by passive diffusion, convection defined by the electric field and by the solute transport when the charge of the drug is negative.

where B is defined by (51). If $B < 0$, then an estimate like (49) holds, replacing C for $|B|$. Otherwise, if $B > 0$ is such that $B\Delta t < 1$ then from (60) we get

$$\left\|c_h^{n+1}\right\|_h^2 \leq \left(\frac{1}{1-\Delta t B}\right)^{n+1} \left\|c_h^0\right\|_h^2, \tag{61}$$

Finally, inequality (52) easily follows from (61).

■

Theorem 5 means that the implicit method (45)-(48) is unconditionally stable when $P_e < 1$ or when $B < 0$. Otherwise, it is conditionally stable.

5. Numerical results

In this section we illustrate the behaviour in different scenarios of the drug concentration in the reservoir and target tissue as well as the released drug. We consider $\ell_1 = 10^{-3}$, $\ell_2 = 2.5 \times 10^{-3}(m)$, for a reservoir with $1(mm)$ of thickness and a target tissue of $1.5(mm)$ of thickness and $A = 1$.

We analyze the dependence on the concentration with the applied potential and the reservoir and target tissue conductivities. The coupled system's parameters (see [3]) are taken as

- $D_r = 10^{-9}(m^2/s)$, $D_s = 10^{-12}(m^2/s)$,
- $\sigma_r = 1.5(S/m)$, $\sigma_s = 0.015(S/m)$,
- $T_r = T_s = 310.15(K)$

and $c(x,0) = 1, x \in (0,\ell_1)$, $c(x,0) = 0, x \in (\ell_1,\ell_2)$. The S.I. units of conductivity are Siemens per meter (S/m).

The scenarios are defined considering the valence z of the diffusion drug equal to -1. The numerical results were obtained using the fully implicit scheme (45)-(48). In Figure 3 we present the concentration profiles for different values of $\delta\phi$, $\delta\phi = 0, 0.02, 0.5, 2$. As $\delta\phi$ increases, the convective rate of transport also increases and consequently, less drug concentration remains in the reservoir and in the target tissue. This behaviour can be observed from the plot of the absorbed mass in Figure 3. We also illustrate the influence of the electric conductivity coefficients. In Figure 4 we plot the drug concentrations and the released mass for $\sigma_s = 0.015$. We observe that a lower electric conductivity in the reservoir can lead to an increase of the released mass. These results were obtained for $\delta\phi = 0.5$.

coupled with the Nernst-Planck equations (1)-(2). Then, for $c_k, k = r, s$, we obtain

$$\begin{cases} \dfrac{\partial c_r}{\partial t} - \nabla\cdot(v_r c_r) = \nabla\cdot(D_r \nabla c_r) \text{ in } (0,\ell_1)\times\mathbb{R}^+, \\ \\ D_r\nabla c_r(0,t) + v_r c_r(0,t) = 0,\ t\in\mathbb{R}^+, \end{cases} \tag{6}$$

and

$$\begin{cases} \dfrac{\partial c_s}{\partial t} - \nabla\cdot((v_s - v_{sol})c_s) = \nabla\cdot(D_s\nabla c_s) \text{ in } (\ell_1,\ell_2)\times\mathbb{R}^+, \\ \\ c_s(\ell_2,t) = 0,\ t\in\mathbb{R}^+. \end{cases} \tag{7}$$

The boundary condition in (6) means that the system is insulated while the boundary condition in (7) states that the drug is immediately removed by the blood stream.

System (6)-(7) is complemented with the interface conditions

$$\begin{cases} c_r(\ell_1,t) = c_s(\ell_1,t) \text{ (continuity of the concentration)}, \\ \\ J_r(\ell_1,t) = J_s(\ell_1,t) \text{ (continuity of the mass flux)}, \end{cases} \tag{8}$$

and the initial condition

$$\begin{cases} c_r(x,0) = c_{r,0},\ x\in(0,\ell_1), \\ \\ c_s(x,0) = 0,\ x\in(\ell_1,\ell_2). \end{cases} \tag{9}$$

Condition (9) means that there is initially a homogeneous drug distribution in the reservoir and that the target tissue is empty.

3. The drug delivery

Solving the potential problems (3), (4) and (5) we easily obtain

$$\begin{cases} \phi_r(x) = \dfrac{\delta\phi}{\ell_1 + \frac{\sigma_r}{\sigma_s}(\ell_2-\ell_1)}x + \phi_0,\ x\in[0,\ell_1], \\ \\ \phi_s(x) = \dfrac{\sigma_r}{\sigma_s}\dfrac{\delta\phi}{\ell_1 + \frac{\sigma_r}{\sigma_s}(\ell_2-\ell_1)}(x-\ell_2) + \phi_1,\ x\in[\ell_1,\ell_2]. \end{cases} \tag{10}$$

where $\delta\phi = \phi_1 - \phi_0$ is the potential difference. From (10) and (2) we deduce the convective velocities

$$\begin{cases} v_r = \dfrac{D_r z F}{RT_r} \dfrac{\delta\phi}{\ell_1 + \frac{\sigma_r}{\sigma_s}(\ell_2 - \ell_1)} \\ v_s = \dfrac{D_s z F}{RT_s} \dfrac{\sigma_r}{\sigma_s} \dfrac{\delta\phi}{\ell_1 + \frac{\sigma_r}{\sigma_s}(\ell_2 - \ell_1)} - v_{sol}. \end{cases} \tag{11}$$

We introduce now the weak formulation of the initial boundary value coupled problem (6), (7), (8) and (9). To do that we define the following space $V = \{w \in H^1(0, \ell_2) : w(\ell_2) = 0\}$.

The weak solution for the previous problem is a function $c \in L^2(\mathbb{R}^+, V) \cap C^1(\mathbb{R}^+, L^2(0, \ell_2))$ such that

$$(c'(t), w) + (vc(t), \nabla w) = -(D\nabla c(t), \nabla w),\ t \in \mathbb{R}^+,\ \forall w \in V, \tag{12}$$

where $(\cdot, \cdot)$ denotes the usual inner product in $L^2(0, \ell_2)$, and

$$c(0) = c_{r,0} \text{ in } [0, \ell_1],\ c(0) = 0 \text{ in } (\ell_1, \ell_2]. \tag{13}$$

Then the drug distribution is defined by

$$c_r(t) = c(t) \text{ in } [0, \ell_1],\ c_s(t) = c(t) \text{ in } [\ell_1, \ell_2].$$

In (12), D and v are defined by

$$D = \begin{cases} D_r,\ x \in (0, \ell_1), \\ D_s,\ x \in (\ell_1, \ell_2), \end{cases} \qquad v = \begin{cases} v_r,\ x \in (0, \ell_1), \\ v_s,\ x \in (\ell_1, \ell_2). \end{cases}$$

To study the stability of the weak problem we recall the following Friedrichs-Poincaré inequality

$$\|w\|^2 \le \frac{\ell_2^2}{2} \|\nabla w\|^2,\ w \in V. \tag{14}$$

An energy estimate for $c(t)$ was established in [6], which we recall in Theorem 1.

Theorem 1. *If $c \in L^2(\mathbb{R}^+, V) \cap C^1(\mathbb{R}^+, L^2(0, \ell_2))$ is a solution of (12), (13) then*

$$\|c(t)\|^2 \le e^{\left(-\frac{1}{\ell_2^2} \min_{k=r,s} D_k + \frac{\max_{k=r,s} v_k^2}{2 \min_{k=r,s} D_k}\right) t} \|c(0)\|^2,\ t \in \mathbb{R}_0^+. \tag{15}$$

From Theorem 1, the stability (as well as uniqueness of solution) of the IBVP (12), (13) can be concluded.

is nonnegative or positive such that $B\Delta t < 1$, then the finite difference scheme (45)-(48) satisfies

$$\|c_h^n\|_h \le e^{n\Delta t \frac{B}{2(1-\Delta t B)}} \left\|c_h^0\right\|_h,\ n = 1, \ldots, N_{\Delta t}, \tag{52}$$

Proof: From (45)-(48) we establish

$$\left\|c_h^{n+1}\right\|_h^2 \le \|c_h^n\|_h^2 - 2\Delta t \min_{k=r,s} D_k \left\|D_{-x} c_h^{n+1}\right\|_{h,+}^2 + 2\Delta t \max_{k=r,s} |v_k| \left\|c_h^{n+1}\right\|_{h,+} \left\|D_{-x} c_h^{n+1}\right\|_{h,+}. \tag{53}$$

(1) $\underline{P_e < 1}$:
Taking into account inequality (34) we get

$$\left\|c_h^{n+1}\right\|_h^2 \le \|c_h^n\|_h^2 + 2\Delta t \left(-\min_{k=r,s} D_k + \max_{k=r,s} |v_k| \ell_2 \right) \left\|D_{-x} c_h^{n+1}\right\|_{h,+}^2. \tag{54}$$

As (38) holds, considering the inequality (33) in (54) we obtain

$$\left\|c_h^{n+1}\right\|_h^2 \le \|c_h^n\|_h^2 - \Delta t B \left\|c_h^{n+1}\right\|_h^2,$$

where $C > 0$ is defined by (50), and consequently

$$\left\|c_h^{n+1}\right\|_h^2 \le \frac{1}{(1 + \Delta t C)^{n+1}} \left\|c_h^0\right\|_h^2. \tag{55}$$

Finally, (49) easily follows from (55).

(2) Other case:
From (53) and (36) it can be shown the following

$$\left\|c_h^{n+1}\right\|_h^2 \le \|c_h^n\|_h^2 - 2\Delta t \min_{k=r,s} D_k \left\|D_{-x} c_h^{n+1}\right\|_{h,+}^2 \tag{56}$$

$$+ 2\Delta t \max_{k=r,s} |v_k| \sqrt{C_{nor}} \left\|c_h^{n+1}\right\|_h \left\|D_{-x} c_h^{n+1}\right\|_{h,+} \tag{57}$$

that leads to

$$\left\|c_h^{n+1}\right\|_h^2 \le \|c_h^n\|_h^2 + \Delta t(-2 \min_{k=r,s} D_k + \epsilon^2) \left\|D_{-x} c_h^{n+1}\right\|_{h,+}^2 \tag{58}$$

$$+ \Delta t \frac{1}{\epsilon^2} \max_{k=r,s} |v_k|^2 C_{nor} \left\|c_h^{n+1}\right\|_h^2, \tag{59}$$

where $\epsilon \neq 0$.
From (58), with $\epsilon^2 = \min_{k=r,s} D_k$, and using (33), we obtain

$$(1 - \Delta t B) \left\|c_h^{n+1}\right\|_h^2 \le \|c_h^n\|_h^2, \tag{60}$$

be the discrete drug mass in the coupled system. Theorem 4 can be used to obtain an estimate for $M_h(t)$. In fact, under condition (38) we have

$$M_h(t) \leq e^{\frac{1}{\ell_2^2}(-\min_{k=r,s} D_k + \ell_2 \max_{k=r,s}|v_k|)t} \|c_h(0)\|_h, \; t \in \mathbb{R}_0^+.$$

We also get a lower estimate for the absorbed mass $M_{abs}(t)$

$$M_{abs}(t) \geq M(0) - e^{\frac{1}{\ell_2^2}(-\min_{k=r,s} D_k + \ell_2 \max_{k=r,s}|v_k|)t} \|c_h(0)\|_h, \; t \in \mathbb{R}_0^+. \tag{44}$$

Let us consider in the integration in time of the semi-discrete problem (26)-(29) the implicit-Euler method. To do that we fix a time interval $[0,T]$ where we introduce a time grid $\{t_n, n = 0, \ldots, N_{\Delta t}\}$ where $t_n - t_{n-1} = \Delta t, n = 1, \ldots, N_{\Delta t}$, and $N_{\Delta t}\Delta t = T$. Let $c_h^n, n = 0, \ldots, N_{\Delta t}$, be defined by

$$\begin{array}{l} c_i^{n+1} = c_i^n + \Delta t D(x_i) D_2 c_i^{n+1} + \Delta t D_c(v_i c_i^{n+1}), \\ i = 0, \ldots, M-1, M, M+1, \ldots, N-1, \\ n = 0, \ldots, N_{\Delta t} - 1, \end{array} \tag{45}$$

$$\begin{cases} D_r D_c c_h^n + M_2(v_r c_h^n) = 0, \; n = 0, \ldots, N_{\Delta t}, \\ c_N^n = 0, \qquad\qquad n = 1, \ldots, N_{\Delta t}, \end{cases} \tag{46}$$

$$\begin{array}{l} D_r D_{-x} c_{M-1/2}^n + M_2\left((v c_h^n)\left(x_{M-1/2}\right)\right) = D_s D_{-x} c_M^n + M_2\left((v_s c_h^n)(x_M)\right), \\ n = 1, \ldots, N_{\Delta t}, \end{array} \tag{47}$$

$$c_i^0 = c_{r,0}, \; i = 0, \ldots, M-1, \; c_i^0 = 0, \; i = M, \ldots, N-1. \tag{48}$$

Under condition (38) we establish in the next result that the fully discrete scheme (45)-(48) is unconditionally stable.

Theorem 5. *If $Pe < \sqrt{2}$ then the numerical concentration c_h^n defined by the implicit finite difference method (45)-(48) satisfies*

$$\|c_h^n\|_h \leq e^{-n\Delta t \frac{C}{2(1+\Delta t C)}} \left\|c_h^0\right\|_h, \; n = 1, \ldots, N_{\Delta t}, \tag{49}$$

where

$$C = \frac{2}{\ell_2^2}\left(\min_{k=r,s} D_k - \max_{k=r,s}|v_k|\ell_2\right). \tag{50}$$

Also, if

$$B = -\frac{1}{\ell_2^2}\min_{k=r,s} D_k + \frac{\max_{k=r,s}|v_k|^2}{\min_{k=r,s} D_k} C_{nor}, \tag{51}$$

The upper bound (15) can be used to study the qualitative behaviour of the drug mass inside of the coupled system and the absorbed drug. Let

$$M(t) = A\int_0^{\ell_2} c(t)\, dx, \; t \in \mathbb{R}_0^+,$$

be the total drug mass in the coupled system, where A represents the area of a square cross section and $\sqrt{A}$ is the distance between the passive and active electrodes, see Figure 2.

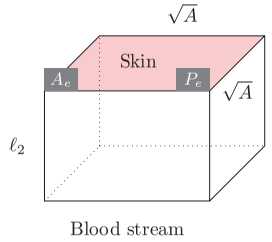

FIGURE 2. Simplified representation of the problem (A_e represents the active electrode and P_e the passive one).

As

$$M(t) \leq \sqrt{\ell_2} A \|c(t)\|,$$

we obtain from Theorem 1 an upper bound for this mass.

Corollary 1. *Under the assumptions of Theorem 1,*

$$M(t) \leq \sqrt{\ell_2} A e^{\left(-\frac{1}{\ell_2^2}\min_{k=r,s} D_k + \frac{\max_{k=r,s} v_k^2}{2\min_{k=r,s} D_k}\right)\frac{t}{2}} \|c(0)\|, \; t \in \mathbb{R}_0^+. \tag{16}$$

Moreover, if

$$\frac{\max_{k=r,s} v_k^2}{\min_{k=r,s} D_k^2} < \frac{2}{\ell_2^2}, \tag{17}$$

then

$$\lim_{t\to\infty} M(t) = 0 \;\; \textit{exponentially.} \tag{18}$$

Let P_e, the Péclet number, be defined by

$$P_e = \frac{\max_{k=r,s}|v_i|}{\min_{k=r,s} D_k}\ell_2.$$

Condition (17) means that if the Péclet number is less than $\sqrt{2}$ then we can easily compute the time level t^* such that the drug mass in the coupled system is less than a positive limit L. In fact, from (16), t^* satisfies

$$t^* \geq \frac{2}{-\frac{1}{\ell_2^2}\min_{k=r,s} D_k + \frac{\max_{k=r,s} v_k^2}{2\min_{k=r,s} D_k}} \ln\left(\frac{L}{A\sqrt{\ell_2}\,\|c(0)\|}\right). \tag{19}$$

As $A\sqrt{\ell_2}\,\|c(0)\|$ represents the initial mass in the system, we always have $L \leq A\sqrt{\ell_2}\,\|c(0)\|$ and consequently, estimate (19) is physically sound.

Let $M_{abs}(t)$ be the absorbed mass at time $t \in \mathbb{R}^+$,

$$M_{abs}(t) = M(0) - M(t).$$

It follows from (16) that

$$M_{abs}(t) \geq M(0) - A\sqrt{\ell_2} e^{\left(-\frac{1}{\ell_2^2}\min_{k=r,s} D_k + \frac{\max_{k=r,s} v_k^2}{2\min_{k=r,s} D_k}\right)\frac{t}{2}} \|c(0)\|, \; t \in \mathbb{R}_0^+. \tag{20}$$

To obtain a second estimate for $M(t)$, we need to improve estimate (15). Taking in (12) $w = c(t)$ we have

$$\frac{d}{dt}\|c(t)\|^2 = -2\left\|\sqrt{D}\nabla c(t)\right\|^2 - 2(vc(t), \nabla c(t)). \tag{21}$$

From (21) we deduce

$$\frac{d}{dt}\|c(t)\|^2 \leq -2\min_{k=r,s} D_k \|\nabla c(t)\|^2 + 2\max_{k=r,s}|v_k|\,\|c(t)\|\,\|\nabla c(t)\|,$$

that leads to

$$\frac{d}{dt}\|c(t)\|^2 \leq \left(-2\min_{k=r,s} D_k + \sqrt{2}\ell_2 \max_{k=r,s}|v_k|\right)\|\nabla c(t)\|^2.$$

Assuming (17) we obtain

$$\frac{d}{dt}\|c(t)\|^2 \leq \left(-2\min_{k=r,s} D_i + \sqrt{2}\ell_2 \max_{k=r,s}|v_k|\right)\frac{2}{\ell_2^2}\|c(t)\|^2,$$

and finally

$$\|c(t)\|^2 \leq e^{\left(-\frac{2}{\ell_2^2}\min_{k=r,s} D_k + \frac{\sqrt{2}}{\ell_2}\max_{k=r,s}|v_k|\right)t}\|c(0)\|^2, \; t \in \mathbb{R}_0^+. \tag{22}$$

From the previous considerations we conclude that under condition (17), we have

$$M(t) \leq A\sqrt{\ell_2} e^{\left(-\frac{2}{\ell_2^2}\min_{k=r,s} D_i + \frac{\sqrt{2}}{\ell_2}\max_{k=r,s}|v_k|\right)\frac{t}{2}}\|c(0)\|, \; t \in \mathbb{R}_0^+. \tag{23}$$

We remark that the previous bound (41) leads to

$$\max_{0\neq u_h\in V_h}\frac{(L_h u_h, u_h)_h}{\|u_h\|_h^2} \leq -\frac{2}{\ell_2^2}\Big(\min_{k=r,s} D_k - \frac{\ell_2}{\sqrt{2}}\max_{k=r,s}|v_k|^2\Big). \tag{42}$$

We recall that the logarithmic norm of the linear operator L_h (or its matrix representation) $\mu[L_h]$ induced by the inner product $(\cdot,\cdot)_h$ is given by

$$\mu[L_h] = \lim_{\tau\to 0^+}\frac{\|I + \tau L_h\|_h - 1}{\tau}$$

and satisfies

$$\mu[L_h] = \max_{0\neq u_h\in V_h}\frac{(L_h u_h, u_h)_h}{\|u_h\|_h^2}.$$

Consequently

$$\mu[L_h] \leq -\frac{2}{\ell_2^2}\Big(\min_{k=r,s} D_k - \frac{\ell_2}{\sqrt{2}}\max_{k=r,s}|v_k|^2\Big).$$

As $c_h(t)$ satisfies (26)-(28), it follows

$$c_h(t) = e^{tL_h}c_h(0), t \geq 0,$$

which leads to

$$\|c_h(t)\|_h \leq \|e^{tL_h}\|_h\|c_h(0)\|_h, t \geq 0.$$

As we have

$$\|e^{tL_h}\|_h \leq e^{-t\frac{2}{\ell_2^2}\left(\min_{k=r,s} D_k - \frac{\ell_2}{\sqrt{2}}\max_{k=r,s}|v_k|^2\right)}, t \geq 0,$$

we obtain the following result:

Theorem 4. *Let $c_h(t)$ be a grid function defined in $I_h^* \cup \{x_{M-1/2}\}$ that satisfies (26)-(29). If (37) and (38) hold then*

$$\|c_h(t)\|_h \leq e^{\frac{2}{\ell_2^2}(-\min_{k=r,s} D_k + \ell_2\max_{k=r,s}|v_k|)t}\|c_h(0)\|_h, t \in \mathbb{R}_0^+. \tag{43}$$

Theorem 4 allow us to conclude the stability of the initial boundary value problem (26)-(29). Let

$$M_h(t) = \frac{h}{4}c_0(t) + \sum_{j=1}^{M-2} hc_j(t) + \frac{3}{4}h\left(c_{M-1}(t) + c_M(t)\right) + \sum_{j=M+1}^{N-1} hc_j(t), \; t \in \mathbb{R}_0^+,$$

that leads to (33).

The proof of inequality (34) follows the same steps.

■

If u_h is defined in $I_h \cup \{x_{M-1/2}$, null at $x = x_N$ and satisfies

$$D_r D_{-x} u_{M-1/2} + v_r M_2 u_h(x_{M-1/2}) = D_s D_{-x} u_M + v_s M_2 u_h(x_M), \tag{35}$$

then

$$\|u_h\|_{h,+}^2 \leq C_{nor} \|u_h\|_h^2, \tag{36}$$

with

$$C_{nor} = \frac{4}{3}\left(1 + 2\frac{\max\{(D_r - \frac{h}{4}v_r)^2, (D_s + \frac{h}{4}v_s)^2\}}{\left(D_r + D_s + \frac{h}{4}(v_r - v_s)\right)^2}\right)$$

provided that h satisfies the following condition

$$D_r + D_s + \frac{h}{4}(v_r - v_s) \neq 0. \tag{37}$$

It can be showed that L_h is nonsingular for a certain class of coupled problems.

Theorem 3. *If*

$$P_e < \sqrt{2}, \tag{38}$$

then the finite difference operator L_h is nonsingular in the space

$V_h = \left\{v_h \text{ defined in } I_h^* \cup \left\{x_{M-1/2}\right\} : D_\eta v_h(x_0) = 0,\ v_h(x_N) = 0,\ v_h \text{ satisfies (35)}\right\}$.

Proof: Using summation by parts we establish

$$(-L_h u_h, u_h)_h \geq \min_{k=r,s} D_k \|D_{-x} u_h\|_{h,+}^2 - (M_2(v v_h), D_{-x} u_h)_{h,+}. \tag{39}$$

We have successively

$$\begin{aligned} -(M_2(v u_h), D_{-x} u_h)_{h,+} &\leq \max_{k=r,s} |v_k| \, \|u_h\|_{h,+} \, \|D_{-x} u_h\|_{h,+} \\ &\leq \frac{\ell_2}{\sqrt{2}} \max_{k=r,s} |v_k| \, \|D_{-x} u_h\|_{h,+}^2. \end{aligned} \tag{40}$$

From (39), (40) and using (33) we get

$$(-L_h u_h, u_h)_h \geq \frac{2}{\ell_2^2}\left(\min_{k=r,s} D_k - \frac{\ell_2}{\sqrt{2}} \max_{k=r,s} |v_k|^2\right) \tag{41}$$

that concludes the proof.

■

As we have

$$\frac{P_e^2}{2} - \sqrt{2} P_e + 1 \geq 0, \quad \forall P_e > 0,$$

we conclude that the upper bound of (16) for the drug mass in the reservoir-target tissue is greater or equal than the upper bound in (23). Furthermore, in this case, the instant t^* such that $M(t) < L$ corresponding to (19) is given by

$$t^* \geq \frac{2}{-\frac{2}{\ell_2^2} \min_{k=r,s} D_k + \frac{\sqrt{2}}{\ell_2} \max_{k=r,s} |v_k|} \ln\left(\frac{L}{A\sqrt{\ell_2}\, \|c(0)\|}\right), \tag{24}$$

where the lower bound in (24) is smaller than the lower bound in (19). From (24) we obtain

$$M_{abs}(t) \geq M(0) - A\sqrt{\ell_2} e^{\left(-\frac{2}{\ell_2^2} \min_{k=r,s} D_k + \frac{\sqrt{2}}{\ell_2} \max_{k=r,s} |v_k|\right)\frac{t}{2}} \|c(0)\|, \, t \in \mathbb{R}_0^+. \tag{25}$$

We finally observe that estimates (20) and (25) can be used to study the dependence of the lower limits for absorbed mass on the parameters that determine the iontophoresis.

4. A discrete model

In this section we present a finite difference method that presents the same qualitative behaviour of the continuous model. We fix a mesh size h in $[0, \ell_2]$ and we define the following grid $I_h = \{x_i,\ i = 0, \ldots, N\}$:

$$x_0 = 0, \quad x_1 = x_0 + \frac{h}{2}, \quad x_i = x_{i-1} + h,\ i = 1, \ldots, N, \quad x_N = \ell_2$$

$$x_{M-1/2} = x_{M-1} + \frac{h}{2}, \quad x_M = \ell_1 + \frac{h}{2},$$

where $\ell_1 = x_{M-1/2}$. Let $x_{-1} = -\frac{h}{2}$. By I_h^* we denote the grid $I_h \cup \{x_{-1}\}$. By D_{-x}, D_c and D_2 we denote the backward, first order centered and second order centered finite difference operators, respectively. By M_4 and M_2 we represent the average operators

$$M_4 v_h(x_j) = \frac{1}{4}\left(v_{j+1} + 2v_j + v_{j-1}\right),\ j = 1, \ldots, N-1,$$

and

$$M_2 v_h(x_j) = \frac{1}{2}\left(v_j + v_{j-1}\right),\ j = 1, \ldots, N,$$

respectively. We consider that $D_2 v_h(x_{M-1})$ is based on a nonuniform grid and defined using the grid points x_{M-2}, x_{M-1} and $x_{M-1/2}$. Similarly, $D_c v_h(x_{M-1})$

is defined using the nonequally spaced grid points x_{M-2} and $x_{M-1/2}$. We also introduce the boundary operator D_η

$$D_\eta v_h(x_0) = D_r D_c v_h(x_0) + v_r M_4 v_h(x_0).$$

Let $c_h(t)$ be a grid function defined in the grid points $I_h^* \cup \{x_{M-1/2}\}$ that satisfies the following system of differential equations

$$c_i'(t) - v(x_i) D_c c_i(t) = D(x_i) D_2 c_i(t),\ i = 0, 1, 2, \ldots, N-1, \tag{26}$$

where $v_k = v_r$, if $i \leq M-1$, and $v_k = v_s$ otherwise, coupled with the following algebraic conditions

$$\begin{cases} D_\eta c_h(t)(x_0) = 0 \\ c_N(t) = 0, \end{cases} \tag{27}$$

$$D_r D_{-x} c_{M-1/2}(t) + v_r M_2 c_h(t)(x_{M-1/2}) = D_s D_{-x} c_M(t) + v_s M_2 c_h(t)(x_M). \tag{28}$$

We assume that at the initial time we have

$$c_i(0) = c_{r,0},\ i = 0, \ldots, M-1,\ c_i(0) = 0,\ i = M, \ldots, N-1. \tag{29}$$

The boundary conditions (27) are the discretizations of the boundary conditions of the differential problem. Moreover, the interface condition (28) is a discrete version of (8). The semi-discete problem (26)-(29) can be rewritten in the following equivalent form

$$\begin{cases} c_h'(t) = L_h c_h(t),\ t > 0, \\ c_h(0) \text{ is defined by (29).} \end{cases} \tag{30}$$

To study the qualitative behaviour of the semidiscrete approximation $c_h(t)$ defined by (30) we introduce now the convenient functional environment following [2].

We introduce the following discrete $L^2(0, \ell_2)$ inner product $(\cdot, \cdot)_h$ for grid functions defined in I_h and null on x_N,

$$\begin{aligned} (u_h, v_h)_h = &\frac{h}{4} u_0 v_0 + \sum_{j=1}^{M-2} h u_j v_j + \frac{3}{4} h u_{M-1} v_{M-1} \\ &+ \frac{3}{4} h u_M v_M + \sum_{j=M+1}^{N-1} h u_j v_j. \end{aligned} \tag{31}$$

By $\|\cdot\|_h$ we denote the norm induced by this inner product. For grid functions defined in $I_h \cup \{x_{M-1/2}\}$ we use the following notations

$$\begin{aligned} (u_h, v_h)_{h,+} = &\frac{h}{2} u_1 v_1 + \sum_{j=2}^{M-1} h u_j v_j + \frac{h}{2} u_{M-1/2} v_{M-1/2} \\ &+ \frac{h}{2} u_M v_M + \sum_{j=M+1}^{N} h u_j v_j. \end{aligned}$$

and

$$\|v_h\|_{h,+} = \sqrt{(v_h, v_h)_{h,+}}.$$

We remark that $(\cdot, \cdot)_h$ and $(\cdot, \cdot)_{h,+}$ satisfy

$$-(D_2 u_h, v_h)_h = (D_{-x} u_h, D_{-x} v_h)_{h,+}, \tag{32}$$

for all grid functions u_h, v_h defined in $I_h^* \cup \{x_{M-1/2}\}$ where u_h and v_h satisfy (27), (28) for $v_r = v_s = 0$. Condition (32) mimics the correspondent continuous relation and it is the basic compatibility requirement for $(\cdot, \cdot)_h$ and $(\cdot, \cdot)_{h,+}$. We observe that existence of the transition point where (28) holds increases the complexity of the analysis and the need of auxiliary results that will have an important role in what follows.

The following discrete Poincaré inequalities have an important role in what follows.

Theorem 2. *For grid functions v_h defined in $I_h \cup \{x_{M-1/2}\}$ and null on the boundary point x_N we have*

$$\|v_h\|_h^2 \leq \ell_2^2 \|D_{-x} v_h\|_{h,+}^2 \tag{33}$$

and

$$\|v_h\|_{h,+}^2 \leq \ell_2^2 \|D_{-x} v_h\|_{h,+}^2. \tag{34}$$

Proof: To simplify the presentation we denote by $h_i, i = 1, \ldots, N+1$, the distance between two consecutive points of the grid $I_h \cup \{x_{M-1/2}\}$. As we have

$$v_j = -\sum_{i=j+1}^{N} h_i D_{-x} v_i, j = 0, \ldots, N-1,$$

we obtain

$$v_j^2 \leq \ell_2 \|D_{-x} v_h\|_{h,+}^2, j = 0, \ldots, N-1,$$